

# XYZ Unsupervised Network: A Robust Image Dehazing Approach

Percy Maldonado-Quispe<sup>a</sup> and Helio Pedrini<sup>b</sup>

*Institute of Computing, University of Campinas, Campinas, SP, 13083-852, Brazil*

**Keywords:** Image Dehazing, Unsupervised Network, Zero-Shot Learning, Disentanglement, Dark Channel Prior, Atmospheric Scattering Model.

**Abstract:** In this work, we examine a major less-explored topic in image dehazing neural networks, specifically how to remove haze (natural phenomenon) in an unsupervised manner from a given image. By considering a hazy image as the entanglement of many “simpler” layers, such as a hazy-free image layer, transmission map layer, and atmospheric light layer, as shown in the atmospheric scattering model, we propose a method based on the concept of layer disentanglement. Our XYZ approach presents improvements in the SSIM and PSNR metrics, this being the combination of the XHOT, YOLY and ZID methods, in which the advantages of each of them are maintained. The main benefits of the proposed XYZ are twofold. First, since it is an unsupervised approach, no clean photos, including hazy-clear pairs, are used as the ground truth. In other words, it differs from the traditional paradigm of deep model training on a large dataset. The second is to consider haze issues as being composed of several layers.

## 1 INTRODUCTION

In bad weather conditions, such as fog and haze, image quality is greatly degraded due to the influence of particles in the atmosphere. The suspended particles will scatter the light and dim the reflected light from the scene, and the scattered atmospheric light will also mix with the light received by the camera and change the contrast and color of the image.

The quality of the images captured by the camera is reduced due to absorption by particles floating in the environment. The phenomenon of degraded image quality on foggy days negatively affects photographic work. The contrast of the image will be reduced and the colors will change. At the same time, the textures and boundaries of objects in the scene become blurred. For vision tasks such as object detection and image segmentation, poor-quality inputs can degrade the performance of well-designed models.


To estimate the global atmospheric light and transmission coefficient per pixel from the atmospheric scattering model, a variety of methods have been proposed, which could be roughly divided into previous assumption-based methods and learning-based methods.


Previous methods rely mainly on some back-

ground derived from the image. For example, Tan (2008) proposed to remove haze by maximizing the local contrast of the image, based on the assumption that clean images tend to have higher contrast. Berman et al. (2016) proposed to remove haze based on the assumption that the colors of an image without haze could well approximate a few hundred colors. Although remarkable performance has been achieved with these methods, the quality of haze removal is highly dependent on the consistency between the data and actual distribution.

To avoid previous assumptions, several authors have devoted much effort to the design of methods based on deep neural networks. This method changes, detects and removes haze from an image by directly learning atmospheric dispersion parameters from the training data. For example, Cai et al. (2016) proposed a convolutional neural network that requires a large set of pairs of clean and haze images, so they are supervised learning methods.

Although supervised learning methods (Qin et al., 2020; Liu et al., 2019; Dong et al., 2020) have achieved high performance in haze removal, they have several limitations, one of which is that they require large-scale clean and fuzzy image pairs to train their models, and such a requirement is usually satisfied by artificially synthesizing fuzzy images, through the physical model with the parameters made

<sup>a</sup>  <https://orcid.org/0009-0007-6391-5370>

<sup>b</sup>  <https://orcid.org/0000-0003-0125-630X>

by hand and the clean image. As pointed out by Golts et al. (2020), synthesized databases are less informative and inconsistent than the real ones. Therefore, it is expected that unsupervised models will be developed.

However, in practice, due to variations in the scene and other factors such as illumination, it is difficult, if not impossible, to collect a large scale dataset with the desired ground truth. As a result, most methods rely on first collecting some clean images and then synthesizing the corresponding hazy images using an atmospheric scattering model with handcrafted parameters. However, when the model trained on the synthetic dataset is applied to real-world haze images, the domain shift problem will arise, as the synthetic haze images are likely to be less informative and inconsistent with the real-world haze images. For this reason, we propose our method called XYZ, which tries to overcome the problems mentioned above. As far as we know, this task was not widely addressed.

As main contributions, we have that our method does not need paired images, that is, we do not have the dependence of having a large data set with images with haze and without haze, which was already a problem in itself. In this work, we propose two approaches in their totality, the first of them is to obtain a simple and lightweight unsupervised neural network (XHOT) for the removal of haze in order to lighten the processing time, on the other hand we have the existing neural network clustering approach for haze removal. XYZ (ZHOT, YOLY and ZID) seeks an integration of the advantages of these methods present in the state of the art, assuming that each method focuses on different aspects such as: Dark Channel Prior approximation, HSV Color Space and the use of a deep neural network such as U-Net.

## 2 RELATED WORK

As a result, many researchers are trying to recover clean, high-quality scenes from haze images. Before the widespread use of deep learning in computer vision tasks, image haze removal algorithms were mainly based on some earlier assumptions (He et al., 2009) and the Atmospheric Scattering Model (ASM) (McCartney, 1978). The processing sequences of these rule-based statistical methods are easy to interpret. However, they can fail when faced with complex real-world scenarios. For example, the popular dark channel prior (He et al., 2009) (DCP) does not handle empty regions well.

The works (Cai et al., 2016; Liu et al., 2019; Zheng et al., 2021) are inspired by deep learning and

combined ASM with convolutional neural networks (CNN) to estimate physical parameters. Quantitative and qualitative experimental results show that deep learning can help predict physical parameters in a supervised manner. Wang et al. (2022a) on the other hand proposes the use of an attention-convolutional module.

Following this, Liu et al. (2019) and Zheng et al. (2021) have demonstrated that end-to-end supervised dehazing networks can be implemented independently of the ASM. Thanks to the powerful feature extraction capability of CNN, these non-ASM-based dehazing algorithms can achieve similar accuracy as ASM-based algorithms.

ASM-based and non-ASM-based supervised algorithms have shown impressive performance. However, they often require synthetic paired images that are inconsistent with real-world hazy images. Therefore, recent research focus on methods that are more suitable to the real world dehazing task. Engin et al. (2018), Li et al. (2020), Golts et al. (2020) and Li et al. (2021) explored unsupervised algorithms that do not require synthetic data.

In addition, Chen et al. (2022) designed a method based on two stages, which eliminates haze using DCP and subsequently optimizes the results using existing features between the transmission and depth map. Wang et al. (2022b) proposes a method completely independent of real haze-free images. However, GAN-based networks have great complexity and runtime.

Data-driven unsupervised dehazing methods have achieved impressive performances. Unlike models that require sufficient data to perform network training, Li et al. (2020) proposed a neural network dehazing process that only requires a single example. They further reduced the dependence of the parameter learning process on data by combining the advantages of unsupervised learning and zero-shot learning.

Methods for unsupervised dehazing that are data-driven have demonstrated outstanding results. In the approaches developed by Li et al. (2020) and Li et al. (2021), a dehazing based on neural networks uses a single example, in contrast to methods that require sufficient data to perform network training. By combining the benefits of unsupervised learning and zero-shot learning, the authors further decreased the dependence of the parameter learning process on data.

Supervised methods of dehazing have achieved excellent results. However, this requires paired data, which is difficult to obtain in the real world. For outdoor scenes with moving objects, it is difficult to guarantee that two images taken on a clear, cloudy day have exactly the same content. This is why other ap-

proaches (Engin et al., 2018; Li et al., 2020; Golts et al., 2020; Li et al., 2021) have explored unsupervised haze removal algorithms.

### 3 UNSUPERVISED APPROACH

In this section, we present the development of our proposed approaches, which combines three unsupervised learning methods. First, there is XHOT 3.1.1, which is based on the fundamentals presented in previous investigations, specifically in the works of (Li et al., 2021) and (Golts et al., 2020). Then, we explore YOLY, based on research by Li et al. (2021), and ZID, based on research by Li et al. (2020). Both methods demonstrated outstanding performance in metrics such as SSIM and PSNR, establishing themselves as state-of-the-art benchmarks in the RESIDE dataset. In addition, it is important to highlight that all the methods described as follows do not require a set of paired images for your training, as they address the removal of haze individually for each image.

#### 3.1 Methods

In the next subsections, we present the methods used in this work, which include XHOT, YOLY and ZID.

##### 3.1.1 XHOT

The XHOT network arises from the need to develop an effective and efficient haze removal solution without relying on paired data, as required in unsupervised learning. Recognizing that haze removal can be broken down into simpler components, we base our strategy on the combination of multiple simple layers, as discussed in previous research (Li et al., 2020).

To address this challenge, we create three neural networks, two of which are convolutional neural networks designed to estimate the best values for  $J(x)$  and  $T(x)$ , respectively, as shown in Figure 1. However, in the case of calculating atmospheric light, an independent component of the image content, we chose to maintain the methodology proposed by previous research, specifically by Li et al. (2020) and Li et al. (2021), who employed a Variational Autoencoder for estimating atmospheric light.

**Architectures.** Three sub-networks were constructed to estimate the values for  $J(x)$ ,  $T(x)$  and  $A$ :

- J-Net: This sub-network consists of a non generative convolutional neural network, which means that it does not alter the dimensions of

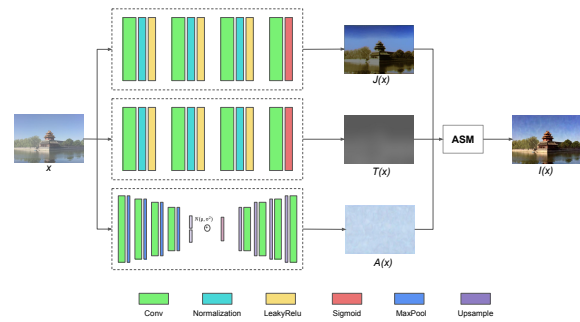


Figure 1: Architecture of our proposed XHOT, in which we have three sub-networks to calculate the variables  $J(x)$ ,  $T(x)$  and  $A$ , respectively.

the input, which is composed of three convolutional blocks, each one performing a convolution with a kernel size 5, followed by normalization by batches and finally a LeakyRelu activation function with a slope of 0.01. At the end of the third block, we applied a convolution together with a Sigmoid activation function, to normalize the output between 0 and 1. The output of this sub-network is an image with 3 channels that is the haze free image  $J(x)$  and that later will be in charge of guiding the training.

- T-Net: This sub-network uses the same neural network as J-Net, however presents a difference with respect to the outcome of the neural network which is a single-channel image, representing the transmission map  $T(x)$  within the image.
- A-Net: This sub-network consists of a Variational Autoencoder, since the variable  $A$  is not related to the content of the image, similar to the work by Li et al. (2020), it is assumed that  $A$  is sampled from a latent Gaussian distribution, and so the problem becomes a variational inference (Kingma and Welling, 2014).

**Loss Function.** To train our unsupervised model, we employ a loss function that combines the loss functions of J-Net and A-Net, as expressed in Equation 1:

$$L_{\text{XHOT}} = L_J + L_A \quad (1)$$

where  $L_J$  is the loss function between the input  $x$  and the result of generating haze  $I(x)$ , this value is calculated taking into account the 3 variables predicted following Equation 2. Then, we can define  $L_J$  as:

$$I(x) = J(x)t(x) + A(1 - t(x)) \quad (2)$$

$$L_J = \text{MSELoss}(I(x), x) \quad (3)$$

In addition, the loss function for the A-Net sub-network is expressed as:

$$L_A = L_H + L_{KL} \quad (4)$$

where  $L_H$  is the loss function  $MSELoss$  between  $A$  and  $A_H$ ,  $A_H$  is the pre-calculated value of the image with haze  $x$  using Dark Channel Prior (He et al., 2009). Finally, the function  $L_{KL}$  is given following the equation 5, where  $KL()$  denotes the Kullback-Leibler divergence between two distributions:

$$\begin{aligned} L_{KL} &= KL(N(\mu_z, \sigma_z^2) || N(0, 1)) \\ &= \frac{1}{2m} \sum_i ((\mu_{z_i})^2 + (\sigma_{z_i})^2 - 1 - \log(\sigma_{z_i}^2)) \quad (5) \end{aligned}$$

### 3.1.2 YOLY

Considering a haze image, represented as  $x$ , the central purpose is to restore the image without haze  $J(x)$  without making use of information beyond what is contained in the image itself. The essence of this method is based on breaking down  $x$  into three sub-networks, as illustrated in Figure 2. To be more precise, YOLY simultaneously channels  $x$  through three main networks: the first is designed to estimate  $J(x)$ , the second to estimate the transmission map  $T(x)$ , and the third focuses on estimating atmospheric light  $A$ . Subsequently, the results of these networks are further combined to reconstruct  $x$  in the upper layer, making use of the atmospheric dispersion model (Equation 2). Therefore, the model as a whole learns in an unsupervised way. In summary, the goal is to minimize the following loss function:

$$L_{rec} = ||I(x) - x|| \quad (6)$$

The cleared image  $J(x)$  is obtained by combining the outputs generated by the three sub-networks, as expressed in Equation 2. The loss function  $L_{rec}$  was designed to regulate the performance of the system as a whole, encompassing both the individual sub-networks and the reconstruction of the haze image  $I(x)$  after calculating its components. More precisely, this loss function monitors and guides the disentangling process, and this is achieved by incorporating the haze generation process.

**Loss Function.** In addition, YOLY proposes a new loss function taking into account the HSV color space, which arises based on the observation made by Zhu et al. (2015), which indicates that the difference between brightness and saturation is close to zero in the haze-free zones. To make use of this previous information, they propose the following equation regarding the prediction of  $J(x)$ .

$$L_J = ||V(J(x)) - S(J(x))|| \quad (7)$$

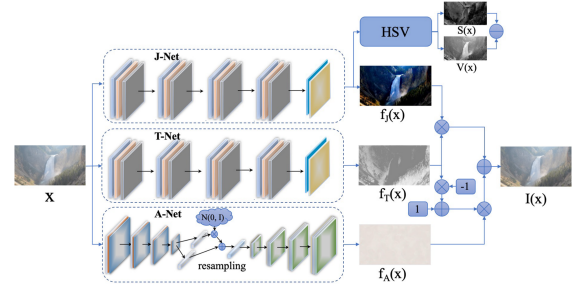


Figure 2: The architecture of YOLY. Extracted from the work developed by Li et al. (2021).

In addition, YOLY proposes a set of loss functions for training the A-Net sub-network, including a regularization function to avoid overfitting.

### 3.1.3 ZID

The approach followed by ZID is similar to YOLY (Li et al., 2021), in terms of deinterlacing the problem into capable simpler ones. However, ZID differs from YOLY in two fundamental respects. First, a distinction is made in terms of the loss function used. Specifically, ZID proposes a loss similar to that used in DCP for J-Net training, while YOLY is based on observing the HSV color space. In addition to this, ZID introduces a smooth regularization in the outputs of T-Net and A-Net, as opposed to YOLY, which only applies this regularization in A-Net. Second, network architectures vary. ZID adopts a structure analogous to the U-Net architecture, in contrast to YOLY, which is based on a non-degenerate architecture.

## 3.2 XYZ Network

In the following subsections, we present the second proposed approach, which is characterized by the integration of the advantages offered by the XHOT, YOLY and ZID methods. It is important to note that the three unsupervised methods retain their respective loss functions, which will play a fundamental role in the training process of the robust model we are proposing.

### 3.2.1 Architecture

As shown in Figure 3, our approach makes use of the methods presented by Li et al. (2020) and Li et al. (2021). As seen in Section 3.1, the proposed methods attempt to deinterlace the effect of haze into layers simpler to calculate, this disentanglement is possible thanks to Equation 2. The atmospheric dispersion model is composed of 3 unknown variables, and that is why the vast majority of dehazing techniques focus

on finding these values. In the same way, XYZ makes use of this disentanglement to be able to calculate the haze free image, that is why our approach has two sub-network groups and one unsupervised neuronal sub-network, the gJ-Net group to calculate the clear image  $J(x)$  and with this to train our neural network with its loss function, gT-Net is in charge of calculating the transmission map  $T(x)$  and finally the sub-network A-Net which estimates the atmospheric light within the image.

- **gJ-Net.** This group is the result of the combination of XHOT, YOLY and ZID methods, where XHOT presents a non-degenerative neural network such as YOLY, which helps us preserve important details for the haze-free image, as it is the case of the object shapes within the image with haze and also preserve the current dimensions. In addition, YOLY makes use of the space of colors HSV to address the training of the unsupervised network. This is thanks to the observations made by Zhu et al. (2015), who formulate that in haze-free areas the difference between brightness and saturation is close to zero. Finally, ZID proposes the training taking into account a loss function based on Dark Channel Prior Loss (Golts et al., 2020), also makes use of a degenerative neural network of the type U-Net with skip connections.
- **gT-Net.** As in J-Net, this sub-network is composed of the three methods seen previously, only with the difference of the output of each method. Independent of the method, they present the transmission map of the image being processed.
- **A-Net.** This sub-network is responsible for calculating the atmospheric light present in an image (independent of the content) so we assume that arises apart from a latent space resulting from a Gaussian distribution, which is why we decided to use only a neural network, specifically a Variational Autoencoder, detailed in Section 3.1.1.

### 3.2.2 Loss Function

To train our model composed of three unsupervised methods, we use together a loss function taking into account the output of each method as described in Equation 8:

$$L_{XYZ} = L_{XHOT} + L_{YOLY} + L_{ZID} \quad (8)$$

where  $L_{XHOT}$  is the loss function for our XHOT method,  $L_{YOLY}$  is the loss function for YOLY and finally  $L_{ZID}$  is the loss function for ZID, we decided to give the same weight to each loss function as the three guide our training, taking into account the assumptions made, such as the case of the HSV color space,

Dark Channel Prior Loss, in addition to the XHOT loss function, which turns out to be an improvement of Golts et al. (2020) and Li et al. (2021).

### 3.3 Datasets

We conducted our experiments using the REAListic Single Image Dehazing (RESIDE) dataset (Li et al., 2019), a well-recognized resource for large-scale haze removal evaluation. This dataset is composed of two test subsets: SOTS and HSTS. The SOTS subset consists of 500 indoor hazy images, which were synthetically generated using a physical model with manually calibrated parameters. In contrast, the HSTS subset contains 10 synthetic hazy images and 10 real-world hazy images captured in diverse scenes. Additionally, the RESIDE dataset offers training subsets: OTS (Outdoor Training Set) comprises a total of 72,135 hazy images generated from 2,061 ground truth images. Meanwhile, ITS (Indoor Training Set) consists of 13,990 hazy images generated from 1,399 ground truth images.

As mentioned previously, the methods described in Section 3.1 do not require a “training” dataset, but only need a set of images to carry out the evaluation of the method. These methods, based on Zero-Shot Learning, eliminate the haze adapting according to the number of iterations made for each image evaluated.

### 3.4 Metrics

To assess the performance of our model, as well as other methods, we employed Structured Similarity Indexing Method (SSIM) and Peak-Signal-to-Noise Ratio (PSNR) (Wang et al., 2004) as image quality analysis metrics, which are commonly used in haze removal studies. SSIM quantifies the structural similarity between the haze-free reference image and the output image obtained from our proposed technique. Similarly, PSNR provides a measure of the relationship between the maximum possible signal power and the noise power present in the images.

These two metrics serve as indicators of the image’s fidelity to the haze-free reference. Models that achieve higher values for these metrics indicate a higher quality and greater similarity between the generated image and the haze-free reference.

## 4 RESULTS

In our experiments, we carry out both qualitative and quantitative assessments, as detailed in Section 3.4.

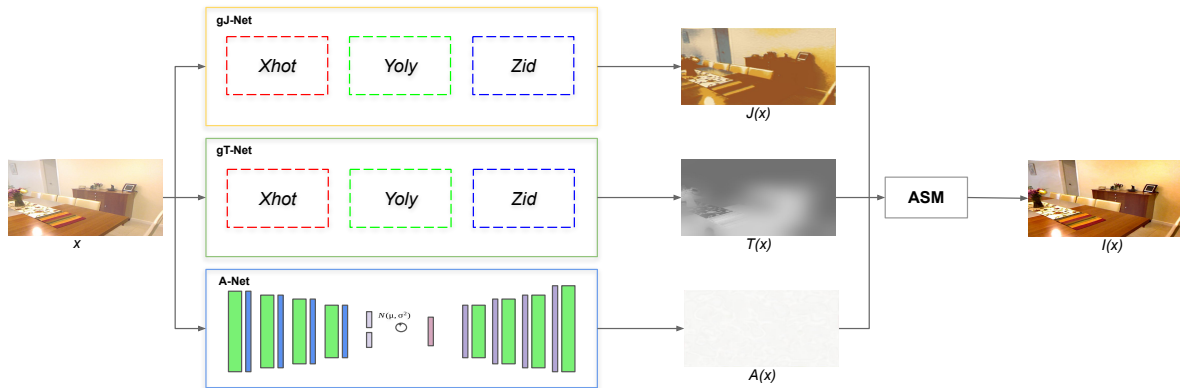


Figure 3: The architecture of our proposed XYZ approach. XYZ includes two groups of sub-networks: gJ-Net group of sub-networks (XHOT, YOLY and ZID) for image estimation clean  $J(x)$ , gT-Net group of sub-networks for transmission map estimation  $T(x)$ . In addition, XYZ maintains layer disentanglement for the estimate of  $A$ .

The test dataset includes manually generated synthetic data as well as actual images provided by Li et al. (2019). These assessments covered a variety of aspects and metrics to provide a comprehensive view of the performance of our imaging haze removal approach.

#### 4.1 Quantitative Comparison

In this section, we present the results by applying our approach of disentanglement of complex layers into simpler layers, compared to the methods proposed by Li et al. (2020) and Li et al. (2021). It is worth mentioning that the methods with which we are making the comparison make use of the disentanglement approach of haze in simpler layers.

As can be seen in Table 1, we can see that our XHOT network does not improve on SSIM and PSNR metrics to ZID and YOLY methods. However, this method still presents significant advances for the elimination of haze. On the other hand, our XYZ network manages to improve the results present in the SOTS data set, which contains images of closed environments in relation to the other HSTS test data set. This still does not improve the other two methods in the metrics. We find it important to clarify that although our technique does not improve the state of the art, this is in the second method with the best result.

#### 4.2 Qualitative Comparison

In this section, we observe the visual results by eliminating haze in outdoor images and in an indoor environment. Figures 4 and 6 show the results achieved by the unsupervised learning-based methods XHOT, ZID (Li et al., 2020), YOLY (Li et al., 2021) and

XYZ, respectively. The images visually show that the results are close to the actual image in terms of color and detail.

From Figure 4, we can observe that the XHOT method presents better results visually in areas such as the sky, since we do not make use directly of an approximation by DCP that normally fails to distinguish the haze from the clouds. On the other hand, ZID presents the most artifacts for the same reason, which uses an approximation by DCP. However, XYZ attempts to make this distinction in a more coherent manner, but still presents artifacts. Figure 5 shows a set of real-world images of the HSTS dataset, from which we can observe that XYZ manages to eliminate the haze in large part of the image with haze, however this still does not manage to eliminate the haze in its entirety.

Figure 6 shows the elimination of haze in closed environments, of which we can observe that the ZID method behaves better in the third image, since it does not lose the details of color in areas such as the floor. However, XYZ achieves better results in images where we have more light as is the case with the first, second and fourth images.

## 5 CONCLUSIONS

In this work, we present an approach to haze removal based on disentanglement of complex layers into simpler layers. We have developed an unsupervised method, called XHOT, which is simple and lightweight. While it is important to note that, to date, this method does not surpass the leading approaches in the state of the art in unsupervised haze removal. Additionally, we propose a group disentanglement approach using three unsupervised methods:

Table 1: Results for XHOT, YOLY, ZID and XYZ methods applied to the SOTS and HSTS datasets. The results are shown in relation to SSIM and PSNR metrics.

Network	SOTS Indoor		HSTS Outdoor	
	SSIM	PSNR	SSIM	PSNR
ZID (Li et al., 2020)	0.815	18.313	<b>0.851</b>	21.650
YOLY (Li et al., 2021)	0.807	17.950	0.832	<b>22.217</b>
XHOT	0.803	17.860	0.829	21.430
XYZ	<b>0.818</b>	<b>18.530</b>	0.846	21.680



Figure 4: Qualitative comparisons on HSTS Outdoor dataset for different methods.



Figure 5: Qualitative comparisons on HSTS Real World for different methods.

XHOT, YOLY and ZID.

This approach, called XYZ, represents an effective strategy that combines the advantages of these three individual methods. XYZ results show significant improvements in image quality metrics, such as SSIM and PSNR, supporting its effectiveness in haze

removal. In other words, both approaches presented in this study address the challenge of haze removal in an unsupervised manner. This is especially valuable as we overcome the limitation of the lack of real-world paired images and eliminate the need to train with an extensive dataset. Our methods address the



Figure 6: Qualitative comparisons on SOTS Indoor dataset for different methods.

haze problem individually for each image, which represents a significant advance in unsupervised haze removal.

## REFERENCES

- Berman, D., Treibitz, T., and Avidan, S. (2016). Non-Local Image Dehazing. In *IEEE Conference on Computer Vision and Pattern Recognition*, pages 1674–1682.
- Cai, B., Xu, X., Jia, K., Qing, C., and Tao, D. (2016). DehazeNet: An End-to-End System for Single Image Haze Removal. *IEEE Transactions on Image Processing*, 25(11):5187–5198.
- Chen, X., Li, Y., Kong, C., and Dai, L. (2022). Unpaired Image Dehazing With Physical-Guided Restoration and Depth-Guided Refinement. *IEEE Signal Processing Letters*, 29:587–591.
- Dong, H., Pan, J., Xiang, L., Hu, Z., Zhang, X., Wang, F., and Yang, M.-H. (2020). Multi-Scale Boosted Dehazing Network With Dense Feature Fusion. In *IEEE/CVF Conference on Computer Vision and Pattern Recognition*, pages 2154–2164.
- Engin, D., Genc, A., and Ekenel, H. (2018). Cycle-Dehaze: Enhanced CycleGAN for Single Image Dehazing. In *IEEE/CVF Conference on Computer Vision and Pattern Recognition Workshops*, pages 938–9388, Los Alamitos, CA, USA. IEEE Computer Society.
- Golts, A., Freedman, D., and Elad, M. (2020). Unsupervised Single Image Dehazing Using Dark Channel Prior Loss. *IEEE Transactions on Image Processing*, 29.
- He, K., Sun, J., and Tang, X. (2009). Single Image Haze Removal Using Dark Channel Prior. In *IEEE Conference on Computer Vision and Pattern Recognition*, pages 1956–1963.
- Kingma, D. and Welling, M. (2014). Auto-Encoding Variational Bayes. *arXiv preprint arXiv:1312.6114*, pages 1–14.
- Li, B., Gou, Y., Gu, S., Liu, J. Z., Zhou, J. T., and Peng, X. (2021). You Only Look Yourself: Unsupervised and Untrained Single Image Dehazing Neural Network. *International Journal of Computer Vision*, pages 1–14.
- Li, B., Gou, Y., Liu, J. Z., Zhu, H., Zhou, J. T., and Peng, X. (2020). Zero-Shot Image Dehazing. *IEEE Transactions on Image Processing*, 29:8457–8466.
- Li, B., Ren, W., Fu, D., Tao, D., Feng, D., Zeng, W., and Wang, Z. (2019). Benchmarking Single-Image Dehazing and Beyond. *IEEE Transactions on Image Processing*, 28(1):492–505.
- Liu, X., Ma, Y., Shi, Z., and Chen, J. (2019). GridDehazeNet: Attention-Based Multi-Scale Network for Image Dehazing. In *International Conference on Computer Vision*.
- McCartney, E. (1978). Optics of the Atmosphere – Scattering by Molecules and Particles. *IEEE Journal of Quantum Electronics*, 14(9):698–699.
- Qin, X., Wang, Z., Bai, Y., Xie, X., and Jia, H. (2020). FFA-Net: Feature Fusion Attention Network for Single Image Dehazing. *AAAI Conference on Artificial Intelligence*, 34(7):11908–11915.
- Tan, R. T. (2008). Visibility in Bad Weather from a Single Image. In *IEEE Conference on Computer Vision and Pattern Recognition*, pages 1–8.
- Wang, E., Shu, S., and Fan, C. (2022a). CNN-based Single Image Dehazing via Attention Module. In *IEEE 5th International Conference on Automation, Electronics and Electrical Engineering*, pages 683–687.
- Wang, Y., Yan, X., Guan, D., Wei, M., Chen, Y., Zhang, X.-P., and Li, J. (2022b). Cycle-SNSPGAN: Towards Real-World Image Dehazing via Cycle Spectral Normalized Soft Likelihood Estimation Patch GAN. *IEEE Transactions on Intelligent Transportation Systems*, 23(11):20368–20382.
- Wang, Z., Bovik, A. C., Sheikh, H. R., and Simoncelli, E. P. (2004). Image Quality Assessment: From Error Visibility to Structural Similarity. *IEEE Transactions on Image Processing*, 13(4):600–612.
- Zheng, Z., Ren, W., Cao, X., Hu, X., Wang, T., Song, F., and Jia, X. (2021). Ultra-High-Definition Image Dehazing via Multi-Guided Bilateral Learning. In *IEEE/CVF Conference on Computer Vision and Pattern Recognition*, pages 16180–16189.
- Zhu, Q., Mai, J., and Shao, L. (2015). A Fast Single Image Haze Removal Algorithm Using Color Attenuation Prior. *IEEE Transactions on Image Processing*, 24(11):3522–3533.